Electronic supplementary materials:

Ultrasensitive Fluorescence Immunoassay for the Detection of Ochratoxin A Using Catalase-Mediated Fluorescence Quenching of CdTe QDs

Xiaolin Huang[1], Shengnan Zhan[1], Hengyi Xu[1], Xianwei Meng[2], Yonghua Xiong[1*], and Xiaoyuan Chen[3*]

[1]State Key Laboratory of Food Science and Technology, Nanchang University, Nanchang 330047, P. R. China;

[2]Laboratory of Controllable Preparation and Application of Nanomaterials, Center for Micro/nanomaterials and Technology, Technical Institute of Physics and Chemistry, Chinese Academy of Sciences, Beijing 100190, P. R. China;

[3]Laboratory of Molecular Imaging and Nanomedicine (LOMIN), National Institute of Biomedical Imaging and Bioengineering (NIBIB), National Institutes of Health (NIH), Bethesda, Maryland 20892, United States

*Correspondence to:

Dr. Yonghua Xiong

State Key Laboratory of Food Science and Technology, and Jiangxi-OAI Joint Research Institute, Nanchang University

Address: 235 Nanjing East Road, Nanchang 330047, P.R. China

Phone: +0086-791-8833-4578. Fax: +0086-791-8833-3708

E-mail: yhxiongchen@163.com

Dr. Xiaoyuan Chen

Laboratory of Molecular Imaging and Nanomedicine (LOMIN), National Institute of Biomedical Imaging and Bioengineering (NIBIB), National Institutes of Health (NIH)

Address: Bethesda, Maryland 20892, United States

Phone: 301-451-4246

E-mail: shawn.chen@nih.gov

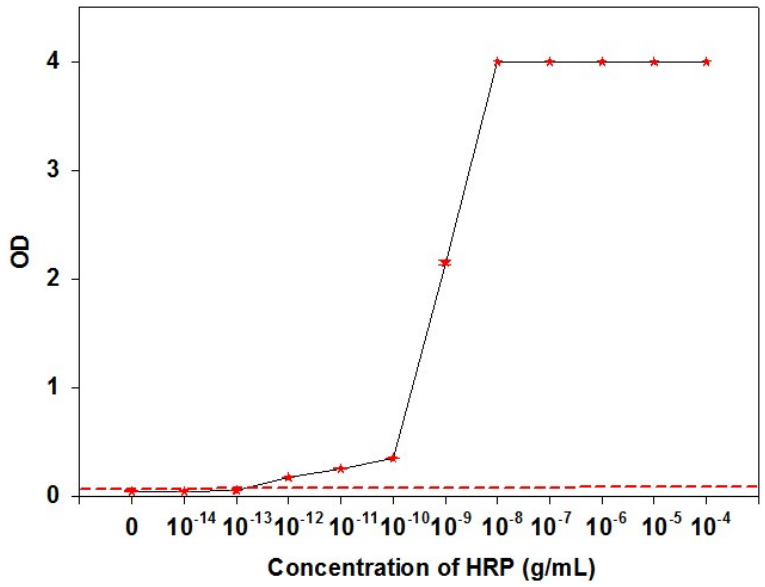

Figure S-1. Absorbance changes upon the interaction of tetramethylbenzidine with different concentrations of HRP ranging from 0 to 10^{-4} g/mL. The red dashed line represents the blank absorbance plus 3 standard deviations. Thus, the LOD of the HRP to tetramethylbenzidine was calculated as 10^{-12} g/mL, which was defined as the lowest concentration of HRP that generated a higher absorbance than the blank absorbance plus 3 standard deviations.

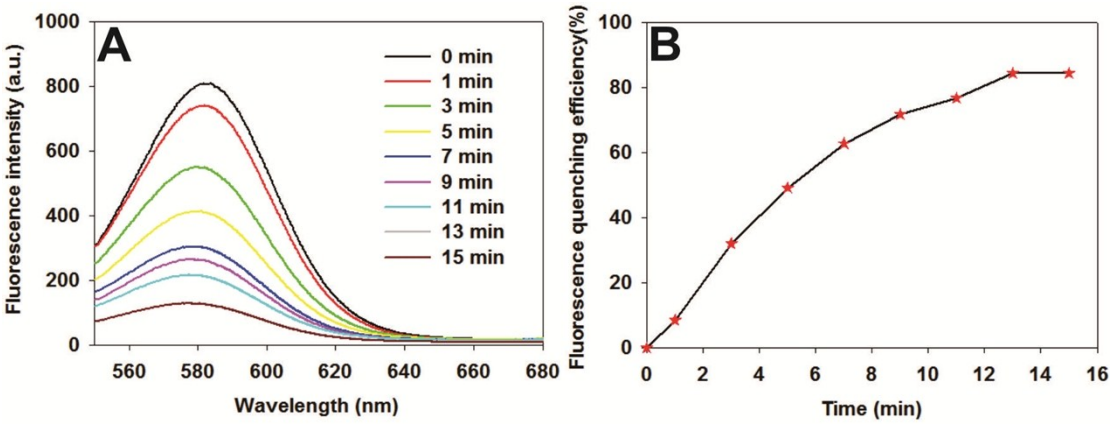

38

39 **Figure S-2**. Typical time-dependent fluorescence changes of CdTe QDs in the

40 presence of 10 μM H_2O_2.

41

42

HRP-based conventional ELISA for OTA detection

96-well polystyrene plates were modified with 100 μL of protein G (20 μg mL^{-1}) in bicarbonate buffer (100 mM, pH 8.6) at 4 °C overnight. After washing three times with washing buffer (PBS, pH 7.4, 0.01 M, containing 0.05% Tween 20), the plates were blocked with blocking buffer (1 mg mL^{-1} of BSA in PBS) for 2 h at 37 °C. After washing three times with washing buffer, 100 μL of anti-OTA mAbs diluted to 1:4000 in PBS were added for 2 h at room temperature. Subsequently, the plates were washed three times with PBST. And then 50 μL $well^{-1}$ of HRP-OTA diluted to 1:400 in PBS was added and incubated with 50 μL $well^{-1}$ of OTA standards with a desired final concentration (0 ng mL^{-1} − 5 ng mL^{-1}) by diluting a stock solution with PB (0.02 M, pH 7.0) containing 5 mM NaCl and 5% methanol. After 1 h at 37 °C, the unbound content was discarded, followed by washing of the microplate three times with washing buffer and twice with PBS. Then, 100 μL of TMB solution was added. After incubation for 15 min at room temperature, the reaction was terminated with 50 μL of 2 M H_2SO_4, and the absorbance was measured at 450 nm using a microplate reader.

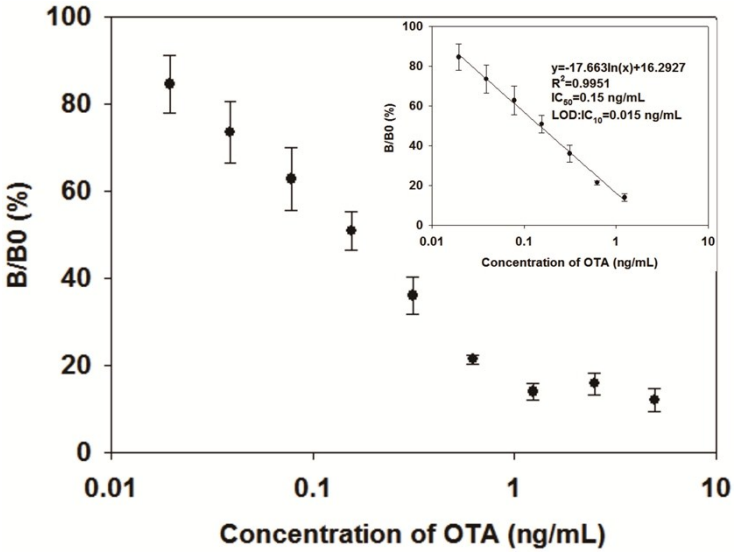

Figure S-3. Quantitative immunoassay of OTA using HRP-based conventional ELISA in spiked PB solution (0.02 M, pH 7) containing 5 mM NaCl and 5% methanol with different concentrations of OTA ranged from 0 ng mL^{-1} to 5 ng mL^{-1}. Vertical bars indicate the standard deviation (n = 3).

Table S1. Checkerboard method for the selection of the working conditions of anti-OTA mAbs and CAT-OTA. The working conditions: mouse anti-OTA mAbs (1.0 mg mL^{-1}) diluted 1:1600 to 1:6400 in coating buffer and CAT-OTA (0.72 mg mL^{-1}) diluted 1:320 to 1:2560 in enzyme dilution buffer. A is the normalized fluorescence intensity of each well in the absence of OTA, B is the normalized fluorescence intensity of each well in the presence of 1.0 ng mL^{-1} OTA, and C is the competitive inhibition rates are obtained by $(1 - F/F_0) \times 100\%$, where F_0 and F represent the normalized fluorescence intensity of the negative sample (OTA-free) and an OTA-spiked PBS solution (1 ng mL^{-1}).

	Dilution of CAT-OTA	Dilution of anti-OTA mAbs		
		1600	**3200**	**6400**
A	**320**	8.5456	6.66714	3.72282
	640	8.17628	6.57454	3.20943
	1280	6.2419	**5.3633**	2.149
	2560	4.518	2.56224	1.30783

	Dilution of CAT-OTA	Dilution of anti-OTA mAbs		
		1600	**3200**	**6400**
B	**320**	4.54284	1.6993	0.81044
	640	3.49164	1.00902	0.33991
	1280	1.44102	**0.2561**	0.07674
	2560	0.5231	0.3363	0.65717

	Dilution of CAT-OTA	Dilution of anti-OTA mAbs		
		1600	**3200**	**6400**
C	**320**	46.84	74.51	78.23
	640	57.30	84.65	89.41
	1280	76.91	**95.22**	96.43
	2560	88.42	86.87	49.75

76
77

Table S2. A comparison of OTA detection performance for nanomaterial-based biosensors.

Signal readout	Nanomaterial	Linear range	Limit of detection	Sample	Ref
SPR	Nanogold hollow balls	0.05 to 7.5 ng mL^{-1}	0.01 ng mL^{-1}	Milk	1
SPR	Gold nanorod	0.04 ng mL^{-1} to 4.03 μg mL^{-1}	0.04 ng mL^{-1}	Corn	2
Colorimetric	Gold nanoparticle	Not available	0.5 ng mL^{-1}	Maize, rice and peanut	3
Colorimetric	Gold nanoparticles	0.05 to 50 ng mL^{-1}	0.009 ng mL^{-1}	Chinese liquor	4
Electrochemistry	Gold nanoparticles	0.1 to 1000 pg mL^{-1}	0.095 pg mL^{-1}	Red wine	5
Electrochemistry	Gold nanoparticles	0.001 to 1 ng mL^{-1}	0.3 pg mL^{-1}	Red wine	6
Electrochemistry	Gold nanoparticles	0.0004 to 20 ng mL^{-1}	0.12 pg mL^{-1}	Red wine	7
Electrochemistry	Magnetic beads	1.3 to 153.8 ng mL^{-1}	0.32 ng mL^{-1}	Coffee	8
Electrochemiluminescence	CdTe quantum dots	0.001 to 20 ng mL^{-1}	0.64 pg mL^{-1}	Red wine	9
Photoelectrochemistry	CdSe nanoparticles	0.01 to 50 ng mL^{-1}	2.0 pg mL^{-1}	Milk	10
Chemiluminescence	Silica nanoparticles	0.001 to 50 ng mL^{-1}	0.3 pg mL^{-1}	Wheat	11
Impedance	Gold nanoparticles	0.04 to 40 ng mL^{-1}	8 pg mL^{-1}	Beer	12
Impedance	Iridium oxide nanoparticles	0.004 to 40 ng mL^{-1}	5.6 pg mL^{-1}	White wine	13
Fluorescence	Upconversion nanoparticles	0.01 to 10 ng mL^{-1}	0.01 ng mL^{-1}	Maize	14
Fluorescence	Silver nanocluster	0.01 to 0.30 ng mL^{-1}	2 pg mL^{-1}	Wheat	15
Fluorescence	Nano-graphite	8 to 160 ng mL^{-1}	8 ng mL^{-1}	Red wine	16
Fluorescence	Europium nanoparticles	Not available	0.05 ng mL^{-1}	Wheat, rice, maize and soybean	17
Fluorescence	Fluorescent nanoparticles	0.04 to 60 ng mL^{-1}	2 pg mL^{-1}	Beer	18
Fluorescence	TiO_2 nanoparticles	0.6 to 403 ng mL^{-1}	0.6 ng mL^{-1}	Beer	19
Fluorescence	Gold nanoparticles	2.5 pg mL^{-1} to 1 μg mL^{-1}	1.4 pg mL^{-1}	Wheat and coffee bean	20
Fluorescence	Single-walled carbon nanohorns	20 to 500 nM	17.2 nM	Red wine	21
Fluorescence	CdTe quantum dots	0.015 to 100 ng mL^{-1}	5.4 pg mL^{-1}	Peanut	22
Fluorescence	CdTe quantum dots	0.05 to 10 pg mL^{-1}	0.05 pg mL^{-1}	Rice, wheat, and corn	This study

Reference:

1 X. H. Fu, *Anal. Lett.*, 2007, **40**, 2641-2652.

2 J.-H. Park, J.-Y. Byun, H. Mun, W.-B. Shim, Y.-B. Shin, T. Li and M.-G. Kim, *Biosens. Bioelectron.*, 2014, **59**, 321-327.

3 X. Li, P. Li, Q. Zhang, R. Li, W. Zhang, Z. Zhang, X. Ding and X. Tang, *Biosens. Bioelectron.*, 2013, **49**, 426-432.

4 Y. Luan, J. Chen, C. Li, G. Xie, H. Fu, Z. Ma and A. Lu, *Toxins (Basel)*, 2015, **7**, 5377-5385.

5 J. Wu, H. Chu, Z. Mei, Y. Deng, F. Xue, L. Zheng and W. Chen, *Anal. Chim. Acta*, 2012, **753**,

27-31.
6 X. Yang, J. Qian, L. Jiang, Y. Yan, K. Wang, Q. Liu and K. Wang, *Bioelectrochemistry*, 2014, **96**, 7-13.
7 S. Xie, Y. Chai, Y. Yuan, L. Bai and R. Yuan, *Biosens. Bioelectron.*, 2014, **55**, 324-329.
8 A. Jodra, M. Hervás, M. Á. López and A. Escarpa, *Sensors Actuators B: Chem.*, 2015, **221**, 777-783.
9 M. Yang, B. Jiang, J. Xie, Y. Xiang, R. Yuan and Y. Chai, *Talanta*, 2014, **125**, 45-50.
10 J. Yang, P. Gao, Y. Liu, R. Li, H. Ma, B. Du and Q. Wei, *Biosens. Bioelectron.*, 2015, **64**, 13-18.
11 X. Hun, F. Liu, Z. Mei, L. Ma, Z. Wang and X. Luo, *Biosens. Bioelectron.*, 2013, **39**, 145-151.
12 G. Evtugyn, A. Porfireva, V. Stepanova, M. Kutyreva, A. Gataulina, N. Ulakhovich, V. Evtugyn and T. Hianik, *Sensors*, 2013, **13**, 16129-16145.
13 L. Rivas, C. C. Mayorga-Martinez, D. Quesada-González, A. Zamora-Gálvez, A. de la Escosura-Muñiz and A. Merkoçi, *Anal. Chem.*, 2015, **87**, 5167-5172.
14 S. Wu, N. Duan, C. Zhu, X. Ma, M. Wang and Z. Wang, *Biosens. Bioelectron.*, 2011, **30**, 35-42.
15 J. Chen, X. Zhang, S. Cai, D. Wu, M. Chen, S. Wang and J. Zhang, *Biosens. Bioelectron.*, 2014, **57**, 226-231.
16 Y. Wei, J. Zhang, X. Wang and Y. Duan, *Biosens. Bioelectron.*, 2015, **65**, 16-22.
17 M. Majdinasab, M. Sheikh-Zeinoddin, S. Soleimanian-Zad, P. Li, Q. Zhang, X. Li, X. Tang and J. Li, *Food Control*, 2015, **47**, 126-134.
18 A. Hayat, R. K. Mishra, G. Catanante and J. L. Marty, *Anal. Bioanal. Chem.*, 2015, **407**, 7815-7822.
19 A. Sharma, A. Hayat, R. K. Mishra, G. Catanante, S. Bhand and J. L. Marty, *Toxins (Basel)*, 2015, **7**, 3771-3784.
20 Y. Liu, J. Yu, Y. Wang, Z. Liu and Z. Lu, *Sensors Actuators B: Chem.*, 2016, **222**, 797-803.
21 L. Lv, C. Cui, C. Liang, W. Quan, S. Wang and Z. Guo, *Food Control*, 2016, **60**, 296-301.
22 C. Wang, J. Qian, K. Wang, K. Wang, Q. Liu, X. Dong, C. Wang and X. Huang, *Biosens. Bioelectron.*, 2015, **68**, 783-790.